Met Office

Report on findings of the CAVIAR consortium on the strength of the infrared water vapour continuum

S. M. Newman

Document history

Date	Version	Comments
6-Mar-2014	1.0	Release to ITWG Sub Group for Radiative Transfer and Surface Property Models

Contents

Introduction

The assimilation of satellite radiances into a numerical weather prediction (NWP) schemes requires the computation of synthetic radiances, which is itself dependent on an accurate knowledge of the spectroscopy of radiatively-active atmospheric species. This is especially important for spaceborne instruments such as the Infrared Atmospheric Sounding Interferometer (IASI) with relatively high spectral resolution (Hilton et al., 2012). The ECMWF/EUMETSAT NWP-SAF Workshop on the assimilation of IASI in NWP[1] recommended that activities aimed at identifying and reducing errors in fundamental spectroscopy should be supported.

Considering applications involving atmospheric humidity, the absorption spectrum of water vapour comprises many thousands of spectral lines, for which the atmospheric transmission is customarily computed using a line-by-line model; the transmission may then be parametrized in a fast model such as RTTOV (Saunders et al., 2002). Models also include an underlying, and relatively smoothly spectrally varying, absorption component known as the water vapour continuum. The physical basis of the continuum has long been the subject of controversy (Ptashnik et al., 2008) and widely-adopted models such as AER's MT_CKD (Clough et al., 2005) adopt a semi-empirical approach which aims to fit the continuum to its observed behaviour. However, these observations are incomplete with the consequence that the dependence of the continuum on temperature and pressure may not be well constrained, and extrapolation to other wavelengths may be problematic.

The Continuum Absorption by Visible and Infrared Radiation and its Atmospheric Relevance (CAVIAR) EPSRC/NERC-funded consortium brought together expertise in atmospheric remote sensing, laboratory measurements and quantum mechanical modelling. The Universities of Reading, Leicester, Cambridge, UCL and Imperial College, together with the Rutherford Appleton Laboratory (RAL), National Physical Laboratory and the Met Office, have coordinated research into the causes and magnitude of the water vapour continuum across the EM spectrum. The consortium concluded its work in 2011, with the resulting deliverables:

1. An improved representation of the strength of continuum absorption suitable for use in radiative transfer models.

2. Improved methodologies for measuring weak absorption in laboratory and field conditions.

[1] http://www.ecmwf.int/publications/library/ecpublications/_pdf/workshop/2009/IASI/WG_reports.pdf

3. An assessment of the impact of the continuum on the present-day and possible future climates.
4. The generation of datasets from theoretical models, lab measurements and field campaigns.

At ITSC-18 the Radiative Transfer and Surface Properties Working Group recommended the CAVIAR findings should be made publicly available in a form suitable for generating reference transmittance training sets (Action RTSP-13). This report summarises the CAVIAR project and details the data formats made available at https://groups.ssec.wisc.edu/groups/itwg/rtsp/refrt.

Theory and definitions

Based on a large body of experimental evidence, the water vapour continuum is differentiated into two components (Clough et al., 1989):

1. **A "self-broadened" component** for which the intensity varies as the square of the water vapour concentration, and is therefore attributed to interactions between pairs of H_2O molecules. Its contribution to the atmospheric spectrum is most apparent in atmospheric "windows" where the optical depth due to other absorbers is small. The self continuum exhibits a strong (negative) temperature dependence.
2. **A "foreign-broadened" component** with a strength proportional to H_2O concentration. This contribution is attributed to interactions between water molecules and "foreign" air molecules, principally N_2 and O_2. The foreign continuum is dominant for "in-band" absorption coinciding with vibration-rotation bands of H_2O lines. The temperature dependence is small (assumed negligible in MT_CKD).

The Clough-Kneizys-Davies (CKD) treatment conveniently defines the continuum as departures of observed absorption strength from that expected from a simple treatment of pressure- and Doppler-broadening for individual spectral lines. Figure 1 illustrates the model as described by Clough et al. (1989). For ease of computation, the Lorentzian part of the line is computed between ± 25 cm^{-1}, and all other water vapour absorption is treated as the continuum. This includes the "plinth" beneath the line at ± 25 cm^{-1} as well as the far wings.

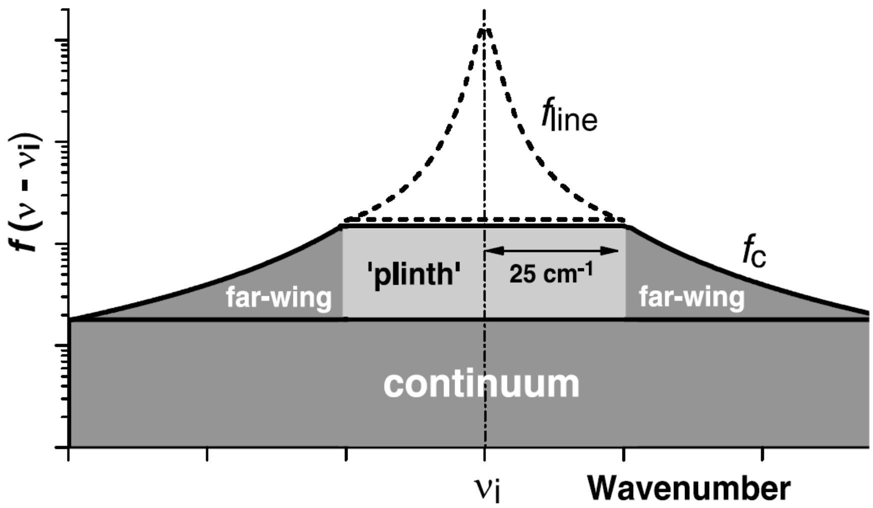

Figure 1. The dashed curve represents the local line contribution (f_{line}), and the solid line the far-wing continuum contribution (f_c), from each spectral line to the total absorption strength in the CKD model. The grey area represents the total continuum absorption, which in the CKD definition includes the far-wing continuum f_c and the 'plinth' (light grey) from under each line within ±25 cm^{-1}. Reproduced from Ptashnik et al. (2011b) Fig. 3.

The CKD continuum coefficients are defined in terms of molecular number density. We can write the total absorption coefficient owing to water vapour (units cm^2 per molecule) as

$$k_{abs}(\nu,T) = R(\nu,T)\left[\left(\frac{\rho_s}{\rho_0}\right)C_s(\nu,T) + \left(\frac{\rho_f}{\rho_0}\right)C_f(\nu,T)\right] + k_{local} \tag{1}$$

as a function of wavenumber (reciprocal wavelength) ν in cm^{-1} and temperature T (K). C_s and C_f are the coefficients for the self and foreign water vapour continua respectively (cm^3 per molecule), ρ_0 is the reference number density at 1 atm and 296 K (molecule cm^{-3}), ρ_s is the density of water vapour and $\rho_f = \rho_0 - \rho_s$ is the foreign gas density (air excluding water vapour). The radiation field term is

$$R(\nu,T) = \nu \tanh\left(\frac{hc\nu}{2k_B T}\right) \tag{2}$$

where h is Planck's constant, c is the speed of light and k_B is Boltzmann's constant. The local line contribution, k_{local}, is defined as a Lorentz line shape for each water vapour line as in Figure 1.

The water vapour self continuum has a long-established strong (negative) temperature dependence. This is expressed in CKD as a function of frequency ν by defining continuum coefficients at 296 K and 260 K and assuming an exponential T-dependence:

$$C_s(\nu,T) = C_s(\nu, 296\,\mathrm{K})\left(\frac{C_s(\nu, 260\,\mathrm{K})}{C_s(\nu, 296\,\mathrm{K})}\right)^{\left(\frac{296\,\mathrm{K}-T}{296\,\mathrm{K}-260\,\mathrm{K}}\right)} \quad (3)$$

By contrast, the water vapour foreign continuum is assumed *T*-independent in CKD.

CAVIAR continuum

By way of an overview, Figure 2 illustrates the strength of the two water vapour components over a broad frequency range, comparing [MT-]CKD model and CAVIAR laboratory room temperature data. It should be noted that the uncertainty in retrieving continuum strengths increases between bands where the continuum is weakest; nevertheless, the CAVIAR results consistently indicated a stronger between-band continuum than MT_CKD-2.4. The self continuum revision in MT_CKD-2.5 corroborated this finding in the 2000-3200 cm^{-1} spectral range.

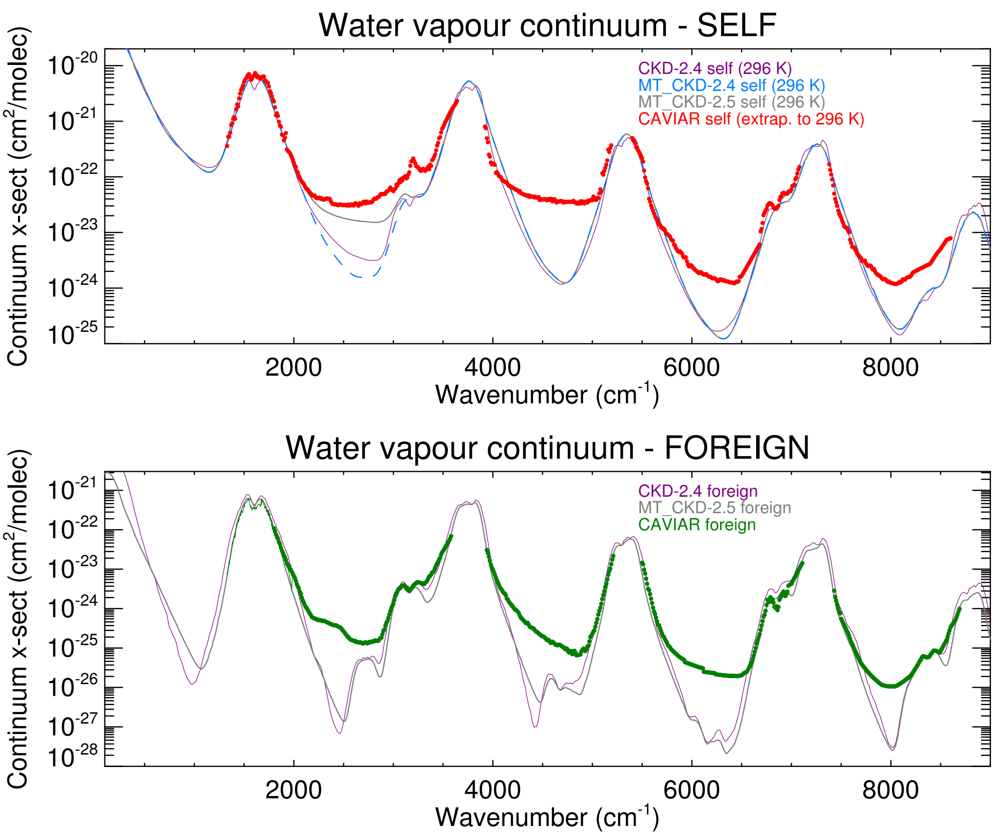

Figure 2. Spectral dependence of the water vapour continuum. Top: self continuum component (absorption cross-section); bottom: foreign continuum component. The continuum strength is shown (see legend) for CKD-2.4 (released 2000), MT_CKD-2.4 (2009) and MT_CKD-2.5 (2010) models (the latter two are identical for the foreign continuum). Also plotted is the continuum strength from RAL laboratory measurements for CAVIAR (Ptashnik et al., 2011(b); Ptashnik et al., 2012).

The CAVIAR results did not extend into the important 800-1200 cm^{-1} atmospheric window, so no firm conclusions can be drawn about the accuracy of models such as MT_CKD in this region. However, this atmospheric window has been the subject of intensive study by many other researchers (see e.g. Baranov et al., 2008) and its temperature dependence is considered adequately constrained by current models.

There has been longstanding disagreement about the conceptual basis of the continuum, and one of the key aims of CAVIAR was to put the continuum on a firmer theoretical footing. Broadly speaking, the different approaches to explaining the origin of the continuum can be divided into two:

1. **Lineshape modification.** In this formulation, the continuum can be explained wholly or mainly as due to departures of the water lineshape from a classical Lorentzian (see e.g. Tipping and Ma, 1995). The non-Lorentzian contributions of many thousands of lines are summed to give an overall continuum.
2. **Dimers.** Here, the self continuum has a large contribution from loosely-bound H_2O-H_2O pairs (dimers). The theoretical dimer spectrum bears many similarities to the experimental self continuum (Daniel et al., 2004) and has the same observed quadratic dependence on H_2O partial pressure.

The CKD (latterly MT_CKD) continuum model relies on lineshape modification, but is "semi-empirical" in that the model is tuned to optimise agreement with observations. This has led to a number of revisions to account for new experimental evidence, for example the "patch" to the self continuum between 2000-3200 cm^{-1} in MT_CKD-2.5 (Figure 2) which increased the continuum strength by an order of magnitude.
It is now computationally feasible to calculate the position and intensity of water dimer absorption features from first principles (see e.g. Kjaergaard et al., 2008). Such *ab initio* calculations predict a number of absorption features that are present in laboratory spectra but absent in models such as MT_CKD (Paynter et al., 2007). The strong consistency of theoretical dimer spectral structures with laboratory results is a key finding of CAVIAR, although the contribution of dimers remains controversial. Ptashnik et al. (2011a) attempt to explain the observed continuum in terms of partitioning of water vapour molecules into free-pair, true bound (stable) and quasi-bound (metastable) dimer states. Without prejudice to the actual continuum mechanism, this report summarises continuum coefficients derived from field and laboratory observations, as an aid to optimising current radiative transfer models.

Field campaign results

The Met Office contribution to CAVIAR comprised field campaign measurements in order to constrain the contribution of the continuum to atmospheric radiation under real atmospheric conditions. The campaign data sets have been used to validate the mid-infrared continuum (Newman et al., 2012a and 2012b), revise the strength of the continuum in the far-infrared spectral region (Green et al., 2012), and investigate the continuum at solar wavelengths (Gardiner et al., 2012). Results pertaining to the mid-infrared spectrum are summarised here.

Continuum in the 2400-3000 cm^{-1} range

The self continuum between 2400-3000 cm^{-1} has undergone a large revision in the most recent version 2.5 of MT_CKD (Figure 3 (a)) to bring the continuum strength into agreement with field datasets (including IASI data, see Mlawer et al., 2012). The new MT_CKD-2.5 coefficients are between 4.8 and 7.4 times larger than in MT_CKD-2.4. CAVIAR laboratory-derived continuum coefficients are slightly larger still.

Figure 3 tests formulations of the continuum against ARIES interferometer measurements from an aircraft case study (tropical atmosphere, see Newman et al., 2012a). By looking upwards at low altitude, ARIES is very sensitive to the water vapour emission again the cold background of space. The LBLRTM (Clough et al., 2005) simulation including MT_CKD-2.4 is unable to reproduce the ARIES brightness temperatures (positive residuals in Figure 3 (c)) whereas MT_CKD-2.5 and the CAVIAR continuum are in much better agreement. The CAVIAR coefficients are not significantly greater than MT_CKD-2.5, given the magnitude of the error bars, between 2400-3000 cm^{-1}, and MT_CKD-2.5 is accepted as being validated in this spectral region.

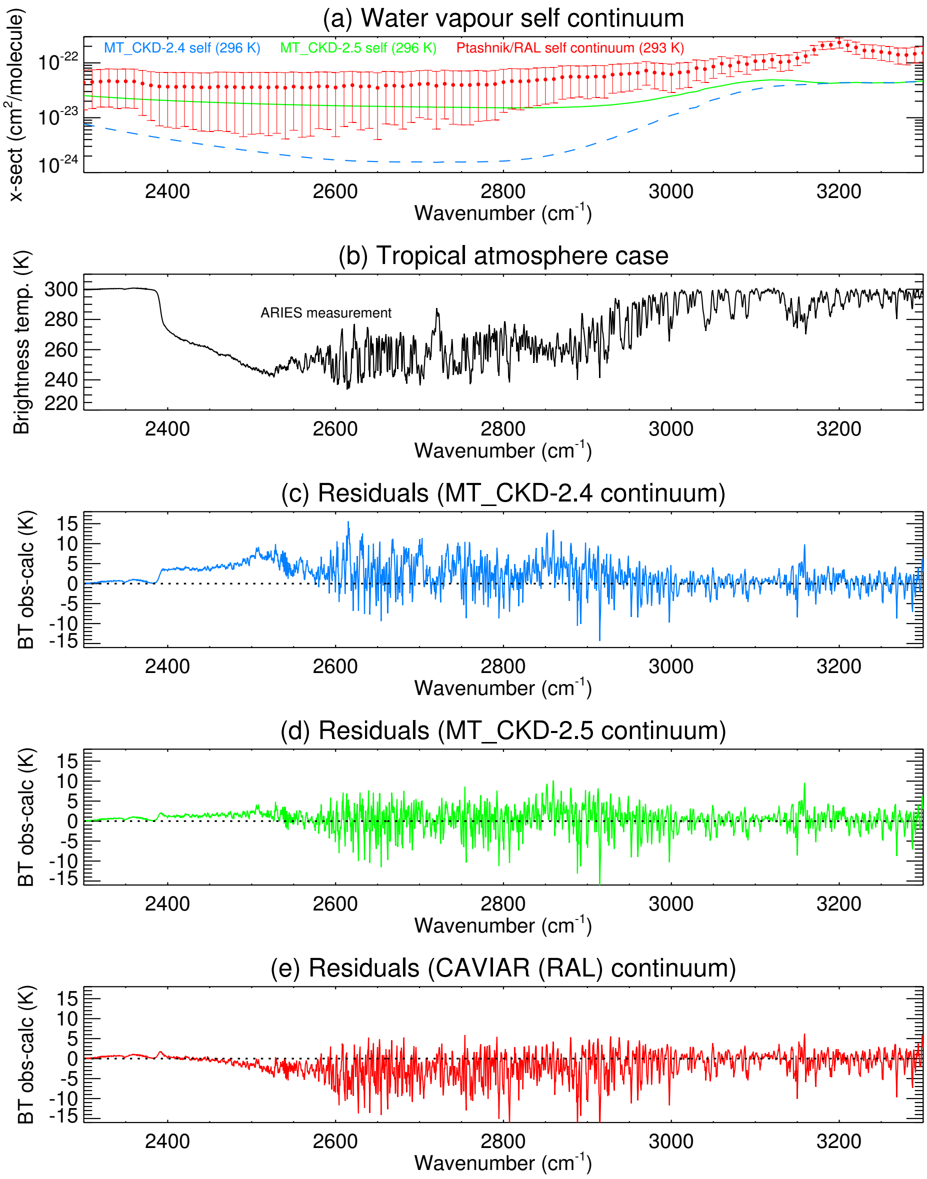

Figure 3. (a) Water vapour self continuum cross-section, at a reference temperature of 296 K, for the MT CKD formulation versions 2.4 (dashed line) and 2.5 (solid line) together with values derived from RAL laboratory data (dotted line with error bars, Ptashnik et al. (2011b)). (b) ARIES upward-looking brightness temperatures from low altitude recorded during the MOTH-Tropic campaign. (c-e) Residual differences (obs−calc) between ARIES and LBLRTM brightness temperatures where the modelled continuum strength is adopted from MT CKD-2.4, MT CKD-2.5 and CAVIAR (RAL) respectively.

Continuum in the 1300-2000 cm^{-1} range

The foreign (mainly H_2O-N_2) continuum has most impact on the atmospheric spectrum within the H_2O vibration-rotation bands, such as that between 1300-2000 cm^{-1} which is used for remote sensing of atmospheric water vapour. Investigation into the foreign continuum strength was a particular focus of the CAVIAR field campaigns. Figure 4 summarises CAVIAR results and those of Rowe and Walden (2009) for the mid-infrared water vapour band (Newman et al., 2012a), compared with MT_CKD-2.5.

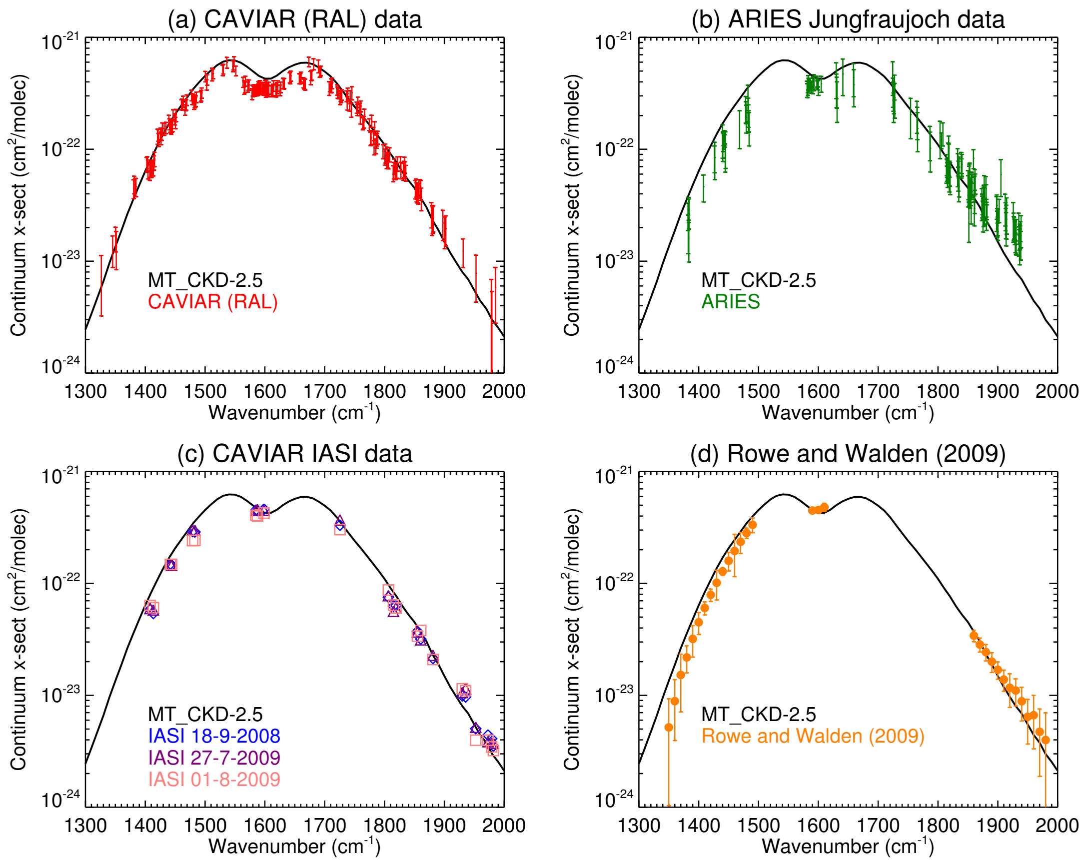

Figure 4. (a) Four determinations of foreign continuum coefficients in the range 1300-2000 cm^{-1}, compared in each case to MT_CKD version 2.5. (a) CAVIAR (RAL) coefficients based on laboratory data at 296 K (Ptashnik et al., 2012); (b) ARIES retrieval from Jungfraujoch CAVIAR flights on FAAM aircraft; (c) IASI derivation from three CAVIAR case studies; (d) Ground-based measurements by Rowe and Walden (2009) in Antarctica corresponding to atmospheric temperatures around –30ºC. Reproduced from Newman et al. (2012a).

Figure 4 (a): The CAVIAR laboratory-derived coefficients, valid at 296 K, show significant deviations from MT_CKD (note the logarithmic scale), particularly near band centre where the CAVIAR continuum strength is smaller.

Figure 4 (b): ARIES upward-looking radiances were used to retrieve the continuum strength from research flights over the Jungfraujoch research station in the Swiss Alps. The height of observation meant that ARIES was sensitive to water vapour emission in the 255-265 K temperature range in the mid-troposphere. ARIES retrieved coefficients were found to be smaller than MT_CKD below 1800 cm^{-1} but comparable to or exceeding MT_CKD above 1800 cm^{-1}.

Figure 4 (c): Continuum coefficients were also retrieved for IASI case studies. The spectral variation in the continuum strength means that the effective temperature of the atmospheric layers contributing to the continuum optical depth is channel-dependent for a nadir-viewing instrument like IASI (Figure 5). Near band centre IASI is sensitive to continuum emission from layers with temperatures near 250 K, whereas near band edges the sensitivity is for layers warmer than 270 K. Near band centre the continuum coefficients retrieved from IASI are in reasonable agreement with MT_CKD.

Figure 4 (d): Ground-based upward-looking interferometer retrievals from Antarctica (independent of CAVIAR), sensitive to the continuum with an effective temperature near 243 K. Deviations relative to MT_CKD are similar to those seen for ARIES.

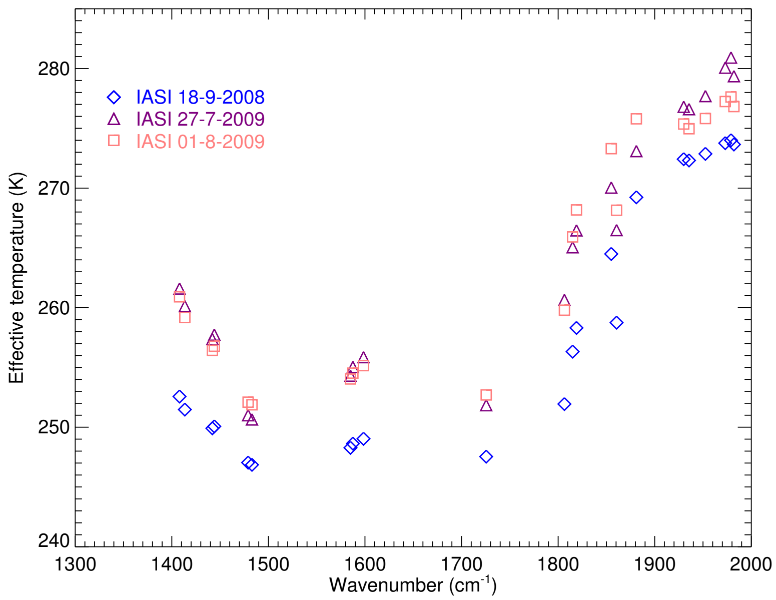

Figure 5. Spectral variation of effective temperatures, as described in Newman et al. (2012a), for IASI continuum-sensitive channels. Data are shown for IASI cases near Camborne, UK on 18 September 2008 (diamonds) and for cases near the Jungfraujoch, Switzerland on 27 July 2009 and 1 August 2009 (triangles and squares respectively).

It has been widely assumed that the water vapour foreign continuum is invariant with temperature: all CKD and MT_CKD models have used a single fixed model for the foreign continuum at all temperatures. There is some evidence from Figure 4 that there may nevertheless be a small *T*-dependent trend in the foreign continuum coefficients. This finding motivates exploring a possible temperature dependency of the foreign continuum strength (next section).

A temperature dependent model of the foreign water vapour continuum

According to Boltzmann's law, the distribution of populated molecular states (and therefore the observed distribution of transitions) will depend on temperature. At lower temperatures states with lower rotational energy will dominate the spectrum, while at higher temperatures more states will be accessed. Figure 6 shows the calculated distribution of H_2O lines at 296 K and 200 K for the 1300-2000 cm^{-1} band. At 200 K the spectrum has greater intensity at band centre, and less near band edges, compared to the 296 K spectrum.

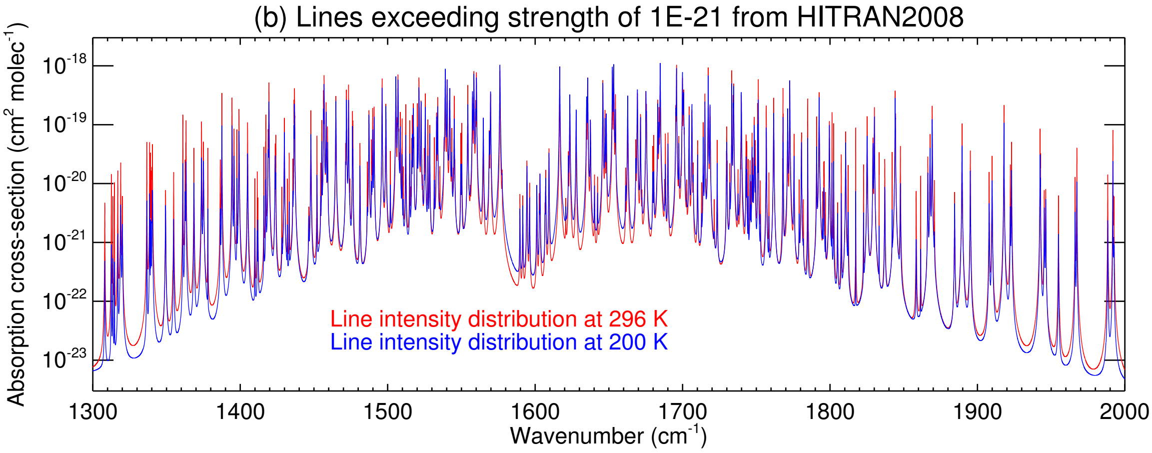

Figure 6. Boltzmann distribution of H_2O line intensities for the strong water band between 1300-2000 cm^{-1}. The simulation has been performed for lines broadened in 1 atm air (cross-section per H_2O molecule) for temperatures of 296 K (red) and 200 K (blue).

Since the foreign (in-band) continuum bears a strong resemblance to a smoothed molecular H_2O line spectrum, we might expect continuum coefficients that are allowed to vary with temperature to show the same kind of behaviour as in Figure 6. It is proposed to model the foreign continuum temperature dependence accounting for changes in rotational line distribution with temperature. We take the CAVIAR laboratory foreign continuum coefficients at 296 K as valid, and perturb the coefficients as a function of temperature in a way consistent with Figure 6. The foreign continuum coefficients are then calculated for any temperature T and wavenumber ν as

$$C_f(\nu,T) = C_f(\nu, 296\,\mathrm{K}) + \left(C_f(\nu, 200\,\mathrm{K}) - C_f(\nu, 296\,\mathrm{K})\right)\left(\frac{T - 296\,\mathrm{K}}{200\,\mathrm{K} - 296\,\mathrm{K}}\right) \quad (4)$$

Extrapolation temperatures of 296 and 200 K were chosen as values encompassing a large part of the tropospheric and stratospheric expected range. At any given frequency a Boltzmann-like perturbation to the continuum strength is approximately linear in temperature (not shown here). Only the mid-infrared H_2O ν2 band foreign coefficients have been extrapolated in temperature.

Validation of temperature dependent model

It is important to test the performance of the *T*-dependent foreign continuum model using case studies where quality-controlled radiance observations and atmospheric profile data are available. Table 1 summarises the case studies investigated – these are all cases where underflights of IASI were carried out with the FAAM research aircraft, i.e. where dropsonde and other profile information can be used to initialise RT simulations.

As noted in LBLRTM validation papers by AER authors Shephard et al. (2009) and Alvarado et al. (2013), some errors in the specification of the atmospheric state are unavoidable, although uncertainties can be minimised through ensuring the remote sensing and profile data sets are very closely collocated in time and space. Following the AER philosophy, for in depth investigation of underlying spectroscopic parameters it is appropriate first to minimise atmospheric state errors through an optimal estimation retrieval. The opposing view is that the minimisation in the retrieval may mask systematic biases in (e.g.) line strengths of a particular molecule.

The approach followed in this report is to show comparisons of IASI observations with simulations based on both “raw” (no retrieval) and “optimised” (retrieved) atmospheric state parameters.

Table 1. Observation data sets used for IASI case studies investigated in this report.

Date [FAAM flight]	Campaign	Location
20/4/2007 [B285]	JAIVEx	Gulf of Mexico (USA)
30/4/2007 [B290]	JAIVEx	Gulf of Mexico (USA)
18/9/2008 [B400]	CAVIAR	Cornish peninsula (UK)
27/7/2009 [B471]	CAVIAR	Jungfraujoch (Switzerland)
1/8/2009 [B473]	CAVIAR	Jungfraujoch (Switzerland)

Figure 7 shows residuals (observed-calculated differences) for each of the case studies summarised in Table 1.

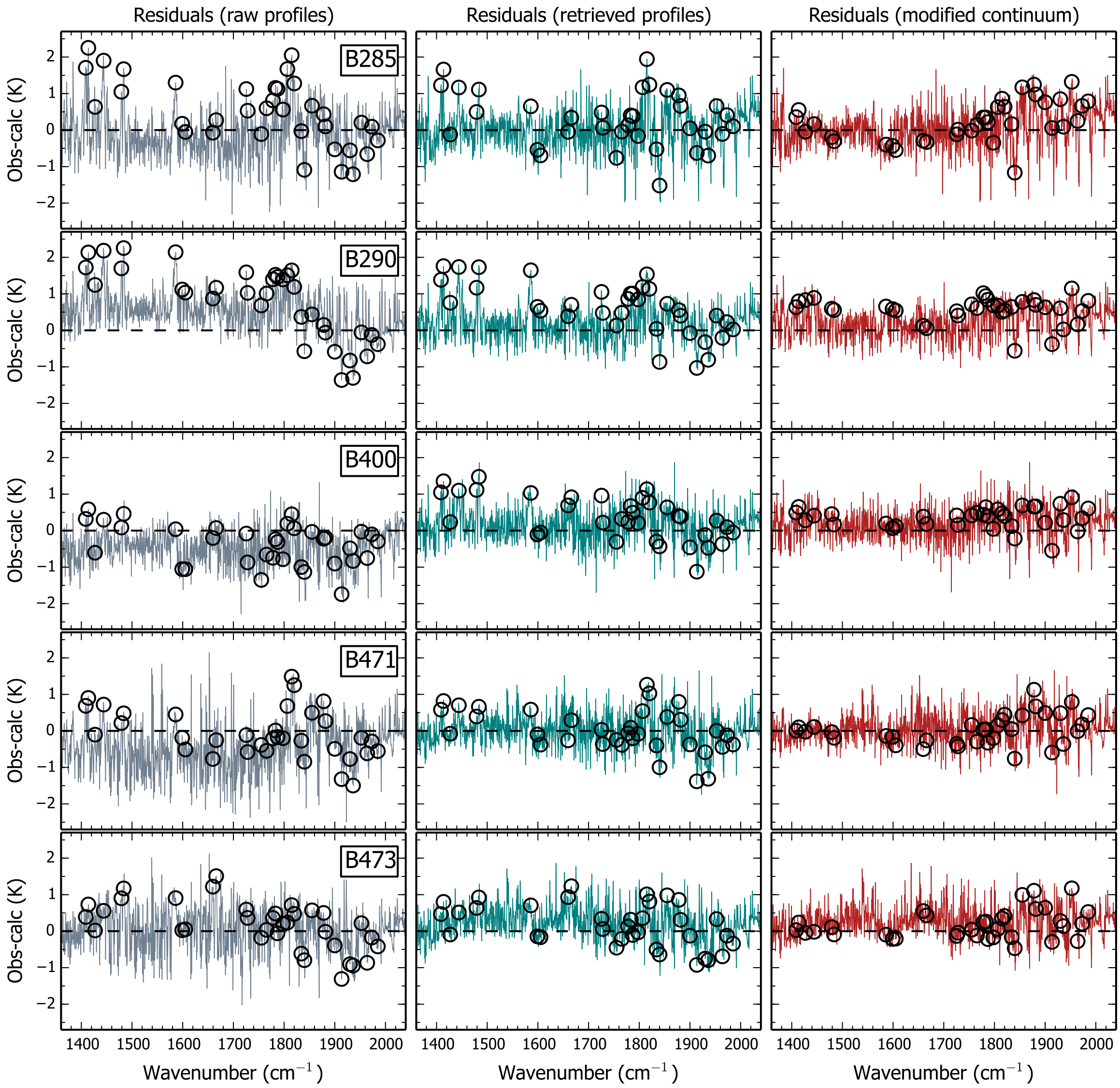

Figure 7. Residual differences (obs-calc brightness temperatures) for each of the five case studies analysed (for each row, see legend and Table 1). Where the case study includes more than one IASI observation, an average residual is plotted. Left column: residuals where best available "raw" profile information has been used as input to LBLRTM in the calculation. Middle column: residuals where a 1d-Var retrieval has been used to estimate a more optimal atmospheric state for input to LBLRTM. Right column: retrieved profile, MT_CKD-2.5 water vapour continuum replaced by the Ptashnik et al. (2011b) self continuum and a modified form of the Ptashnik et al. (2012) foreign continuum where a temperature dependence has been introduced. The circled data points denote those IASI channels with particular sensitivity to the water vapour continuum.

Three sets of residuals are shown:

1. Residuals calculated using LBLRTM version 12.1 with the best available atmospheric profile information (e.g. from dropsondes and aircraft in situ measurements) used as input to the line-by-line calculation. The profile data are "raw", i.e. unmodified.
2. A 1d-Var step is performed for each IASI observation in order to retrieve a more optimal temperature and humidity profile. The background error covariance matrix in the retrieval is derived from correlations within the ensemble of profile measurements for each case, and contains cross-covariances between temperature and humidity.

The observation error is approximated by the IASI spectral noise (diagonal matrix). The resulting retrieved profile is input to LBLRTM to regenerate the residuals.

3. A modified version of LBLRTM is used where the Ptashnik et al. (2011b, 2012) self/foreign water vapour continua are substituted for the MT_CKD formulation and additionally the foreign continuum has a temperature-dependent component as suggested from the Met Office CAVIAR research. The retrieved profile from the 1d-Var step is used in the calculations.

As expected, the raw profile data sets are imperfect, resulting in departures from zero in the spectral residuals across the water vapour sounding band. The 1d-Var retrieval (middle column in Figure 7) succeeds in reducing the residual biases – however, of the remaining large residuals many are identified (circled) as continuum-sensitive channels. Using a modified continuum improves the residual fit across much (though not all) of the spectral range shown in Figure 7.

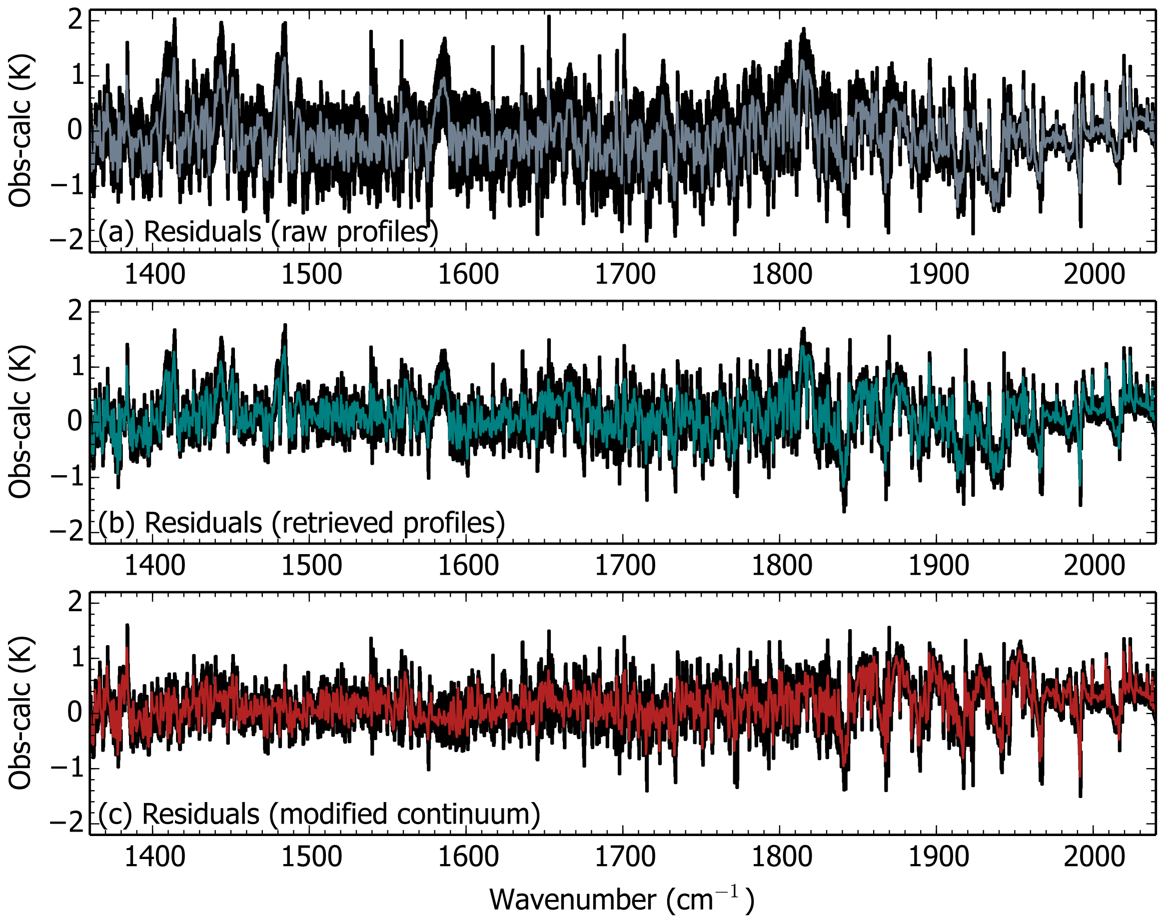

Figure 8. Mean and standard deviation of obs-calc residuals as shown in Figure 7. The coloured lines represent the spectral mean, while the black bars represent the standard deviation over the five cases. (a) Raw profile used in LBLRTM, (b) retrieved profile, (c) retrieved profile and modified water vapour continuum.

The same data are replotted in Figure 8 as mean residuals across the strong water vapour band. A modified continuum model makes a positive change to the magnitude of some residuals in the 1400-1700 cm^{-1} range; between 1800-2050 cm^{-1} the residuals remain large, however, and may be related to uncertainties in the collisional physics affecting the core lineshape.

Data provided to ITWG

Data files uploaded to the Radiative Transfer and Surface Properties Working Group website at https://groups.ssec.wisc.edu/groups/itwg/rtsp are documented in Table 2. These are provided "as is": they are a reference data set for RT simulations and are not intended as a direct replacement for existing continuum models.

AER's LBLRTM is generally considered the reference forward model for atmospheric thermal radiance simulations, and the LBLRTM-format continuum files are provided here for users' convenience. However, these files are in no way endorsed by AER and do not represent an official code release. They may not be compatible with future releases of LBLRTM.

The modified LBLRTM continuum coefficients are tabulated at 1 cm^{-1} resolution (rather than 10 cm^{-1} in MT_CKD) in order to capture the spectral dependence of the laboratory-derived data. This does not appear to impinge on the calculation speed. The H_2O foreign continuum coefficients differ from MT_CKD-2.5 only in the range 1327.0 to 1985.0 cm^{-1}. The self continuum coefficients have been modified over the range 1281.75 to 3500.0 cm^{-1}.

A note on unit conversions: the coefficients in units of cm^3 per molecule are defined according to the CKD definition (Equation 1). By convention, in LBLRTM the radiation field term is subsumed into the coefficients and a scaling of 1×10^{20} is applied.

Table 2. CAVIAR related data files made available to ITWG by the Met Office. For further information about the EPSRC/NERC-funded consortium project see **http://www.met.reading.ac.uk/caviar/**. For information about the Rutherford Appleton Laboratory Molecular Spectroscopy Facility see **http://www.stfc.ac.uk/ralspace/24992.aspx**.

File	Description
Ptashnik_data_selfcon_JGR_2011.dat	Self (H_2O-H_2O) continuum coeffcients published by Ptashnik et al. (2011b), tabulated for the 2010-9550 cm^{-1} range. Data were obtained from measurements at the Rutherford Appleton Laboratory (RAL), UK.
Ptashnik_data_selfcon_JQSRT_2013.dat	Self continuum coeffcients published by Ptashnik et al. (2013), tabulated for the 1314-6901 cm^{-1} range. Data were obtained from measurements at the Institute of Atmospheric Optics, Tomsk, Russia.
Ptashnik_data_foreign_PTRSA_2012.dat	Foreign (H_2O-X, where X represents foreign gas molecules found in air) continuum coeffcients published by Ptashnik et al. (2012) for the 2010-8940 cm^{-1} range. Data were obtained from measurements at RAL.
Ptashnik_RAL-MSF_1300-1900cm-1_H2O-foreign_296K_and_310K.dat	Foreign continuum coefficients partly unpublished but the subject of analysis in Newman et al. (2012a). Data are provided for the 1310-1980 cm^{-1} range. Data were obtained from measurements at RAL.
contnm.f90.caviar	Modified LBLRTM version 12.1 continuum subroutine. Water vapour continuum coefficients (self at 296 K and 260 K, foreign at 296 K) have been substituted by CAVIAR data where available. Additionally, the foreign continuum is made temperature dependent by introducing coefficients extrapolated to 200 K according to the Met Office scheme.

Acknowledgements

Thanks to Igor Ptashnik for supplying continuum coefficients retrieved from laboratory spectra, and Ed Pavelin, Fiona Smith and Nigel Atkinson for assisting with IASI operational data. Airborne data were obtained using the BAe 146-301 Atmospheric Research Aircraft flown by Directflight Ltd, and managed by the Facility for Airborne Atmospheric Measurements, which is a joint entity of the Natural Environment Research Council (NERC) and the Met Office. This work was supported by the EPSRC/NERC CAVIAR consortium.

References

Alvarado, M. J., V. H. Payne , E. J. Mlawer , G. Uymin , M. W. Shephard, K. E. Cady-Pereira , J. S. Delamere1, and J.-L. Moncet (2013), Performance of the line-by-line radiative transfer model (LBLRTM) for temperature, water vapor, and trace gas retrievals: recent updates evaluated with IASI case studies, Atmospheric Chemistry and Physics Discussions, 13, 79–144.

Baranov, Y. I., W. J. Lafferty, Q. Ma, and R. H. Tipping (2008), Water-vapor continuum absorption in the 800-1250 cm^{-1} spectral region at temperatures from 311 to 363 K, Journal of Quantitative Spectroscopy & Radiative Transfer, 109(12-13), 2291-2302.

Clough, S. A., F. X. Kneizys and R. W. Davies (1989), Line shape and the water vapour continuum, Atmospheric Research, 23, 229-241.

Clough, S. A., M. W. Shephard, E. Mlawer, J. S. Delamere, M. Iacono, K. Cady-Pereira, S. Boukabara, and P. D. Brown (2005), Atmospheric radiative transfer modeling: a summary of the AER codes, Journal of Quantitative Spectroscopy & Radiative Transfer, 91(2), 233-244.

Daniel, J. S., S. Solomon, H. G. Kjaergaard, and D. P. Schofield (2004), Atmospheric water vapor complexes and the continuum, Geophysical Research Letters, 31(6).

Gardiner, T. D., M. Coleman, H. Browning, L. Tallis, I. V. Ptashnik, and K. P. Shine (2012), Absolute high spectral resolution measurements of surface solar radiation for detection of water vapour continuum absorption, Philosophical Transactions of the Royal

Society a-Mathematical Physical and Engineering Sciences, 370(1968), 2590-2610, doi:10.1098/rsta.2011.0221.

Green, P. D., S. M. Newman, R. J. Beeby, J. E. Murray, J. C. Pickering, and J. E. Harries (2012), Recent advances in measurement of the water vapour continuum in the far-infrared spectral region, Philosophical Transactions of the Royal Society A-Mathematical Physical and Engineering Sciences, 370(1968), 2637-2655, doi:10.1098/rsta.2011.0263.

Hilton, F., R. Armante, T. August et al. (2012), Hyperspectral Earth Observation from IASI: five years of accomplishments, Bulletin of the American Meteorological Society (to be published March 2012).

Kjaergaard, H. G., A. L. Garden, G. M. Chaban, R. B. Gerber, D. A. Matthews, and J. F. Stanton (2008), Calculation of vibrational transition frequencies and intensities in water dimer: Comparison of different vibrational approaches, Journal of Physical Chemistry A, 112(18), 4324-4335.

Mlawer, E. J., V. H. Payne, J.-L. Moncet, J. S. Delamere, M. J. Alvarado, and D. D. Tobin (2012), Development and recent evaluation of the MT_CKD model of continuum absorption, Philosophical Transactions of the Royal Society A (accepted for publication).

Newman, S. M., P. D. Green, I. V. Ptashnik, T. D. Gardiner, M. D. Coleman, R. A. McPheat, and K. M. Smith (2012a), Airborne and satellite remote sensing of the mid-infrared water vapour continuum, Philosophical Transactions of the Royal Society A-Mathematical Physical and Engineering Sciences, 370(1968), 2611-2636, doi:10.1098/rsta.2011.0223.

Newman, S. M., A. Larar, W. L. Smith, I. Ptashnik, R. Jones, M. Mead, H. Revercomb, D.Tobin, Joe Taylor, and Jonathan Taylor (2012b), The Joint Airborne IASI Validation Experiment: an evaluation of instrument and algorithms, Journal of Quantitative Spectroscopy and Radiative Transfer (accepted for publication).

Paynter, D. J., I. V. Ptashnik, K. P. Shine, and K. M. Smith (2007), Pure water vapor continuum measurements between 3100 and 4400 cm^{-1}: Evidence for water dimer absorption in near atmospheric conditions, Geophysical Research Letters, 34(12), 5.

Ptashnik, I. V. (2008), Evidence for the contribution of water dimers to the near-IR water vapour self-continuum, Journal of Quantitative Spectroscopy & Radiative Transfer, 109(5), 831-852.

Ptashnik, I. V., K. P. Shine, and A. A. Vigasin (2011a), Water vapour self-continuum and water dimers: 1. Analysis of recent work, Journal of Quantitative Spectroscopy & Radiative Transfer, 112(8), 1286-1303.

Ptashnik, I. V., R. A. McPheat, K. P. Shine, K. M. Smith, and R. G. Williams (2011b), Water vapor self-continuum absorption in near-infrared windows derived from laboratory measurements, Journal of Geophysical Research-Atmospheres, 116.

Ptashnik, I. V., R. A. McPheat, K. P. Shine, K. M. Smith, and R. G. Williams (2012), Water vapour foreign-continuum absorption in near-infrared windows from laboratory measurements, Philosophical Transactions of the Royal Society A-Mathematical Physical and Engineering Sciences, 370(1968), 2557-2577, doi:10.1098/rsta.2011.0218.

Ptashnik, I. V., T. M. Petrova, Y. N. Ponomarev, K. P. Shine, A. A. Solodov, and A. M. Solodov (2013), Near-infrared water vapour self-continuum at close to room temperature, Journal of Quantitative Spectroscopy & Radiative Transfer, 120, 23-35, doi:10.1016/j.jqsrt.2013.02.016.

Rowe, P. M., and V. P. Walden (2009), Improved measurements of the foreign-broadened continuum of water vapor in the 6.3 μm band at -30ºC, Applied Optics, 48(7), 1358-1365.

Saunders, R. W., M. Matricardi, P. Brunel, S. J. English, and G. Deblonde (2002), RTTOV-7: A satellite radiance simulator for the new millennium, Proceedings of ITSC-XII, Lorne, Australia, 28 February – 5 March.

Shephard, M. W., S. A. Clough, V. H. Payne, W. L. Smith, S. Kireev, and K. E. Cady-Pereira (2009), Performance of the line-by-line radiative transfer model (LBLRTM) for temperature and species retrievals: IASI case studies from JAIVEx, Atmospheric Chemistry and Physics, 9(19), 7397-7417.

Tipping, R. H., and Q. Ma (1995), Theory of the water-vapor continuum and validations, Atmospheric Research, 36(1-2), 69-94.

Met Office
FitzRoy Road, Exeter
Devon EX1 3PB
United Kingdom

Tel: 0870 900 0100
Fax: 0870 900 5050
enquiries@metoffice.gov.uk
www.metoffice.gov.uk